axioms

MDPI

Article

High-Order Compact Difference Method for Solving Two- and Three-Dimensional Unsteady Convection Diffusion Reaction Equations

Jianying Wei , Yongbin Ge * and Yan Wang

School of Mathematics and Statistics, Ningxia University, Yinchuan 750021, China; weiwy2002@163.com (J.W.); wangyan9370169@163.com (Y.W.)
* Correspondence: gyb@nxu.edu.cn

Abstract: In this paper, a type of high-order compact (HOC) finite difference method is developed for solving two- and three-dimensional unsteady convection diffusion reaction (CDR) equations with variable coefficients. Firstly, an HOC difference scheme is derived to solve the two-dimensional (2D) unsteady CDR equation. Discretization in time is carried out by Taylor series expansion and correction of the truncation error remainder, while discretization in space is based on the fourth-order compact difference formulas. The scheme is second-order accuracy in time and fourth-order accuracy in space. The unconditional stability is obtained by the von Neumann analysis method. Then, this scheme is extended to solve the three-dimensional (3D) unsteady CDR equation. It needs only a five-point stencil for 2D problems and a seven-point stencil for 3D problems. Moreover, the present schemes can solve the nonlinear Burgers equation. Finally, numerical experiments are conducted to show the good performances of the new schemes.

Keywords: convection diffusion reaction equation; two- and three-dimensional equations; variable coefficients; high-order compact difference method; unconditionally stable numerical method

Citation: Wei, J.; Ge, Y.; Wang, Y. High-Order Compact Difference Method for Solving Two- and Three-Dimensional Unsteady Convection Diffusion Reaction Equations. *Axioms* **2022**, *11*, 111. https://doi.org/10.3390/axioms11030111

Academic Editor: Maya Briani

Received: 17 January 2022
Accepted: 1 March 2022
Published: 3 March 2022

1. Introduction

The CDR equation is a kind of basic mathematical physics equation, which is usually used to describe many physical and chemical processes. It has wide applications in ecological environment, fluid mechanics, biological mathematics, and other fields of natural science. For example, the CDR equation has been used to describe the following: the conduction of heat in the fluid [1], thermo-hygro transfer in porous media [2], predator–prey interactions in population densities [3], the transport of adsorbing contaminants and microbe–nutrient systems in groundwater [4], heat transfer in a draining film [5], etc. However, in most cases, similar to some other widely used mathematical models [6,7], the CDR equation cannot obtain exact solutions. So, how to get effective and accurate numerical solutions of this kind of equation is always a problem that researchers pay attention to.

For different model equations, researchers will use different numerical methods. For example, a local discrete exterior calculus discretization [8] of the convection diffusion equation for compressible and incompressible flow is proposed, and the discretization needs to be stabilized by introducing artificial diffusion. For the CDR equation, the numerical methods mainly include finite element method [9–14], integration factor method [15–18], meshless method [1,19], finite difference (FD) method [20–28], and so on. Among them, the FD method is a traditional numerical method, which has been widely used in solving various fluid dynamic equations for a long time [29]. In the past decades, the HOC FD method has been used and developed rapidly because of its various advantages, such as higher accuracy, smaller grid stencils, good stability, etc. For instance, through a new treatment for the reaction term, a high-accuracy FD scheme was given in [21] for solving the one-dimensional (1D) steady CDR problem with a small diffusivity ε; then, the scheme

was extended to the 2D problem with the alternating direction technique. Tong et al. [22] proposed two fourth-order methods by using a second-order scheme followed by the Richardson extrapolation and a direct fourth-order FD scheme for a steady CDR equation with variable coefficients. Jha and Singh [23] formulated an HOC scheme for the 3D steady CDR equation with variable coefficients, which exhibits third to fourth-order accuracy depending on exponential expanding and compact difference approximation. Blended compact FD schemes with fourth- and sixth-order accuracy were developed for solving the 3D CDR equation with mixed derivatives in [24], which require a 19-point compact stencil for the interior gird points. For unsteady case, an unconditionally stable compact method for solving the 1D equation was devised in [25], whose truncation error is $O(\tau^2 + h^4)$ (τ is the time step length and h is the space step length). In addition, for 1D problem, another scheme with fourth-order accuracy in both temporal and spatial directions was proposed in [26], which is transformed into a reaction diffusion equation and is unconditionally stable. In [27], Zhu and Rui presented an adaptive difference strategy with high accuracy for the 1D CDR equation, which explains the nonlinear singular quenching phenomena of the degradation. A local 1D scheme for solving a 2D CDR equation (the parabolic problem) has been presented in [28]. The scheme has second-order accuracy in time and fourth-order accuracy in space.

More HOC FD schemes have been used to solve unsteady convection diffusion equations. In [30], Noye and Tan established a five-point HOC FD scheme with a large stability region. The truncation error of the scheme is $O(\tau^2 + h^3)$. An HOC FD scheme [31] was devised for the 2D variable convection coefficients equation, which is fourth-order in space and not more than second-order in time according to weighted discretization. In addition, for the 2D problem, Karaa and Zhang [32] proposed a fourth-order alternating direction implicit (ADI) scheme, which produces an efficient solver by using 1D tridiagonal algorithm, and the unconditional stability is proved by discrete Fourier analysis. Tian and Ge [33] derived a compact ADI scheme by using a spatial discrete exponential fourth-order compact difference formula and the Crank–Nicolson (C-N) format for the time discretization. Tian [34] also proposed another unconditionally stable rational compact ADI difference method. This method is unconditionally stable too, and compared with [32], it has a smaller dissipation error and better resolution properties, while both schemes have the same order. Li et al. [4] formulated a fourth-order compact scheme of the 2D equation to solve groundwater pollution problems, which is also unconditionally stable. Sun and Lenard [35] proposed a six-order scheme by using a combined compact difference scheme for the spatial discretization and the C-N scheme for the temporal discretization. Although the scheme is sixth-order in space, it is only second-order in time, so to match the sixth-order accuracy in space, a very small time step-length must be adopted in the calculation. The schemes in [4,30,32–35] are only applicable to constant coefficients problems. For the 3D problem, Karaa [36] derived an HOC-ADI method, but the unconditional stability is only suitable for the diffusion case, while the stability of the convection diffusion case is conditionally stable. Another HOC-ADI method was given by Cao and Ge [37], which is also fourth order in space and second order in time, and this method is unconditionally stable. In addition, Ge et al. [38,39] presented an exponential high-order compact ADI method and a rational high-order compact ADI method, respectively, which have a 27-point stencil. These two methods have the same accuracy order and stability as the method in [37]. However, the above methods [36–39] are also only suitable for constant coefficients problems. From the above, we find that most of these HOC methods for 2D or 3D unsteady convection diffusion equations are only applicable to constant coefficients cases. This is also especially true for the CDR equation. So, the intention of this work is to develop an HOC method to solve the variable coefficients case, which is worthy of further study.

We attempt to develop a type of HOC difference method for two- and three-dimensional unsteady CDR equations with variable coefficients in this paper. The second-derivative terms in space are converted to the first-derivative terms by using the fourth-order compact difference approximations. The fourth-order Padé schemes are employed to explicitly

compute the first derivatives. The truncation error remainder correction method is used to discretize the temporal derivative term. The derivation process is simple, and it does not require discrete convection terms as some previous works do. In this way, compact difference schemes with temporally second-order and spatially fourth-order accuracy can be obtained by using the minimum grid points. However, since the first-derivative terms need to be solved coupled with the unknown function, the computational cost is relatively high. The remainder of this study is arranged into four sections. In Section 2, an HOC difference scheme is proposed to solve the 2D CDR equation. The truncation error of this scheme is $O(\tau^2 + h_x^4 + h_y^4)$, and von Neumann linear stability analysis is also conducted in this part. Then, the scheme will be extended to the 3D CDR equation in Section 3. Numerical experiments are carried out to obtain approximate results in Section 4; at the same time,we will compare them with those in the literature to demonstrate the accuracy and stability. Finally, concluding remarks are given in Section 5.

2. 2D CDR Equation

Firstly, we consider the 2D unsteady CDR equation [14,18] with variable coefficients as follows:

$$u_t + p(x,y,t)u_x + q(x,y,t)u_y + c(x,y,t)u = \alpha(u_{xx} + u_{yy}) + f(x,y,t),\ (x,y) \in \Omega,\ t \geq 0, \quad (1)$$

with initial and boundary conditions

$$u(x,y,0) = g(x,y),\ (x,y) \in \Omega, \quad (2)$$

$$u(x,y,t) = s(x,y,t),\ (x,y) \in \partial\Omega,\ t > 0. \quad (3)$$

where $\Omega = \{(x,y) : a_1 \leq x \leq b_1, a_2 \leq y \leq b_2\}$, a_1, a_2, b_1, and b_2 are constants, $\partial\Omega$ is the boundary of Ω. α is the constant diffusion coefficient ($\alpha > 0$); $p(x,y,t)$ and $q(x,y,t)$ are convection coefficients in x- and y- directions, respectively. $c(x,y,t)$ is the reaction coefficient, which is non-negative. p, q, c and exterior force f are regular enough, and their required derivatives exist. We assume that $g(x,y)$ and $s(x,y,t)$ are known functions of sufficient smoothness and satisfy the compatibility condition $s(x,y,0) = g(x,y)$ for $(x,y) \in \partial\Omega$ such that the initial-boundary value Problem (1)–(3) owns a unique solution.

2.1. HOC Difference Scheme

In order to establish HOC difference scheme of model Equation (1), we divide the domain Ω into uniform mesh. In the x- direction: $a_1 = x_0, x_1, x_2, \cdots, x_{N_x} = b_1$, in the y- direction: $a_2 = y_0, y_1, y_2, \cdots, y_{N_y} = b_2$, with the space step length $h_x = x_i - x_{i-1}, 1 \leq i \leq N_x$ and $h_y = y_j - y_{j-1}, 1 \leq j \leq N_y$, τ represents the time step length, $t_n = n\tau, 0 \leq n \leq M$. The discretization of $u(x,y,t)$ at point (x_i, y_j, t_n) is expressed as $u_{i,j}^n$. Define the difference operators as follows:

$$\delta_x u_{i,j}^n = \frac{u_{i+1,j}^n - u_{i-1,j}^n}{2h_x},\ \delta_x^2 u_{i,j}^n = \frac{u_{i+1,j}^n - 2u_{i,j}^n + u_{i-1,j}^n}{h_x^2}, \quad (4)$$

$$\delta_y u_{i,j}^n = \frac{u_{i,j+1}^n - u_{i,j-1}^n}{2h_y},\ \delta_y^2 u_{i,j}^n = \frac{u_{i,j+1}^n - 2u_{i,j}^n + u_{i,j-1}^n}{h_y^2}. \quad (5)$$

For Equation (1), take the value at the (n)th time level and adopt fourth-order Padé difference formulas [40] to calculate u_x and u_y as follows:

$$\frac{1}{6}(u_x)_{i-1,j} + \frac{2}{3}(u_x)_{i,j} + \frac{1}{6}(u_x)_{i+1,j} = \frac{u_{i+1,j} - u_{i-1,j}}{2h_x} + O(h_x^4), \quad (6)$$

$$\frac{1}{6}(u_y)_{i,j-1} + \frac{2}{3}(u_y)_{i,j} + \frac{1}{6}(u_y)_{i,j+1} = \frac{u_{i,j+1} - u_{i,j-1}}{2h_y} + O(h_y^4). \quad (7)$$

while u_{xx} and u_{yy} are approximated by the following fourth-order compact formulas:

$$(u_{xx})_{i,j}^n = 2\delta_x^2 u_{i,j}^n - \delta_x (u_x)_{i,j}^n + O(h_x^4), \tag{8}$$

$$(u_{yy})_{i,j}^n = 2\delta_y^2 u_{i,j}^n - \delta_y (u_y)_{i,j}^n + O(h_y^4). \tag{9}$$

then Equation (1) is written as

$$\begin{aligned}(u_t)_{i,j}^n = {} & 2\alpha\delta_x^2 u_{i,j}^n - \alpha\delta_x (u_x)_{i,j}^n + 2\alpha\delta_y^2 u_{i,j}^n - \alpha\delta_y (u_y)_{i,j}^n \\ & - p_{i,j}^n (u_x)_{i,j}^n - q_{i,j}^n (u_y)_{i,j}^n - c_{i,j}^n u_{i,j}^n + f_{i,j}^n + O(h_x^4 + h_y^4).\end{aligned} \tag{10}$$

Using the Taylor series expansion, we have

$$(u_t)_{i,j}^n = \delta_t^+ u_{i,j}^n - \frac{\tau}{2}(u_{tt})_{i,j}^n + O(\tau^2), \tag{11}$$

in which, $\delta_t^+ u_{i,j}^n = \frac{u_{i,j}^{n+1} - u_{i,j}^n}{\tau}$. To improve the accuracy in the time direction, u_{tt} in Equation (11) needs to be processed. So, we take the derivative of both sides of Equation (1) for t to get

$$u_{tt} = \alpha(u_{xxt} + u_{yyt}) - p_t u_x - p u_{xt} - q_t u_y - q u_{yt} - c_t u - c u_t + f_t. \tag{12}$$

Then, in Equation (12), we use the first-order forward difference to discretize the time derivative term and adopt Equations (6)–(9) to calculate the first and second-derivative terms in spatial direction, respectively, we have

$$\begin{aligned}(u_{tt})_{i,j}^n = {} & 2\alpha\delta_t^+\delta_x^2 u_{i,j}^n - \alpha\delta_t^+\delta_x (u_x)_{i,j}^n + 2\alpha\delta_t^+\delta_y^2 u_{i,j}^n - \alpha\delta_t^+\delta_y (u_y)_{i,j}^n \\ & - \delta_t^+ p_{i,j}^n \cdot (u_x)_{i,j}^n - p_{i,j}^n \delta_t^+ (u_x)_{i,j}^n - \delta_t^+ q_{i,j}^n \cdot (u_y)_{i,j}^n - q_{i,j}^n \delta_t^+ (u_y)_{i,j}^n \\ & - \delta_t^+ c_{i,j}^n \cdot u_{i,j}^n - c_{i,j}^n \delta_t^+ u_{i,j}^n + \delta_t^+ f_{i,j}^n + O(\tau + h_x^4 + h_y^4),\end{aligned} \tag{13}$$

we can get

$$\begin{aligned}(u_t)_{i,j}^n = {} & \delta_t^+ u_{i,j}^n - \tau\alpha\delta_t^+\delta_x^2 u_{i,j}^n + \frac{\tau\alpha}{2}\delta_t^+\delta_x (u_x)_{i,j}^n - \tau\alpha\delta_t^+\delta_y^2 u_{i,j}^n + \frac{\tau\alpha}{2}\delta_t^+\delta_y (u_y)_{i,j}^n \\ & + \frac{\tau}{2}\delta_t^+ p_{i,j}^n \cdot (u_x)_{i,j}^n + \frac{\tau}{2} p_{i,j}^n \delta_t^+ (u_x)_{i,j}^n + \frac{\tau}{2}\delta_t^+ q_{i,j}^n \cdot (u_y)_{i,j}^n + \frac{\tau}{2} q_{i,j}^n \delta_t^+ (u_y)_{i,j}^n \\ & + \frac{\tau}{2}\delta_t^+ c_{i,j}^n \cdot u_{i,j}^n + \frac{\tau}{2} c_{i,j}^n \delta_t^+ u_{i,j}^n - \frac{\tau}{2}\delta_t^+ f_{i,j}^n + O(\tau^2 + \tau h_x^4 + \tau h_y^4).\end{aligned} \tag{14}$$

Finally, by substituting Equation (14) into Equation (10) and omitting the higher-order terms, we get

$$\begin{aligned}& \delta_t^+ u_{i,j}^n - \tau\alpha\delta_t^+\delta_x^2 u_{i,j}^n + \frac{\tau\alpha}{2}\delta_t^+\delta_x (u_x)_{i,j}^n - \tau\alpha\delta_t^+\delta_y^2 u_{i,j}^n + \frac{\tau\alpha}{2}\delta_t^+\delta_y (u_y)_{i,j}^n + \frac{\tau}{2}\delta_t^+ p_{i,j}^n \cdot (u_x)_{i,j}^n \\ & + \frac{\tau}{2} p_{i,j}^n \delta_t^+ (u_x)_{i,j}^n + \frac{\tau}{2}\delta_t^+ q_{i,j}^n \cdot (u_y)_{i,j}^n + \frac{\tau}{2} q_{i,j}^n \delta_t^+ (u_y)_{i,j}^n + \frac{\tau}{2}\delta_t^+ c_{i,j}^n \cdot u_{i,j}^n + \frac{\tau}{2} c_{i,j}^n \delta_t^+ u_{i,j}^n - \frac{\tau}{2}\delta_t^+ f_{i,j}^n \\ & = 2\alpha\delta_x^2 u_{i,j}^n - \alpha\delta_x (u_x)_{i,j}^n + 2\alpha\delta_y^2 u_{i,j}^n - \alpha\delta_y (u_y)_{i,j}^n - p_{i,j}^n (u_x)_{i,j}^n - q_{i,j}^n (u_y)_{i,j}^n - c_{i,j}^n u_{i,j}^n + f_{i,j}^n.\end{aligned} \tag{15}$$

Equation (15) is the present HOC difference scheme for solving the 2D unsteady variable coefficient CDR Equation (1), in which we adopt consistent fourth-order formulas [41] to calculate the values at the boundary points of u_x and u_y

$$\begin{aligned}(u_x)_{0,j} + \frac{14}{15}(u_x)_{1,j} = {} & \frac{1}{h_x}\Big(-\frac{184}{75}u_{0,j} + \frac{703}{180}u_{1,j} - \frac{89}{30}u_{2,j} \\ & + \frac{67}{30}u_{3,j} - \frac{77}{90}u_{4,j} + \frac{41}{300}u_{5,j}\Big), (j = 0, 1 \cdots, N_y),\end{aligned} \tag{16}$$

$$(u_y)_{i,0} + \frac{14}{15}(u_y)_{i,1} = \frac{1}{h_y}(-\frac{184}{75}u_{i,0} + \frac{703}{180}u_{i,1} - \frac{89}{30}u_{i,2} + \frac{67}{30}u_{i,3} - \frac{77}{90}u_{i,4} + \frac{41}{300}u_{i,5}), (i = 0, 1, \cdots, N_x), \tag{17}$$

$$(u_x)_{N_x,j} - \frac{14}{15}(u_x)_{N_x-1,j} = \frac{1}{h_x}(\frac{52}{25}u_{N_x,j} - \frac{1067}{180}u_{N_x-1,j} + \frac{67}{10}u_{N_x-2,j} - \frac{41}{10}u_{N_x-3,j} + \frac{133}{90}u_{N_x-4,j} - \frac{69}{300}u_{N_x-5,j}), (j = 0, 1 \cdots, N_y), \tag{18}$$

$$(u_y)_{i,N_y} - \frac{14}{15}(u_y)_{i,N_y-1} = \frac{1}{h_y}(\frac{52}{25}u_{i,N_y} - \frac{1067}{180}u_{i,N_y-1} + \frac{67}{10}u_{i,N_y-2} - \frac{41}{10}u_{i,N_y-3} + \frac{133}{90}u_{i,N_y-4} - \frac{69}{300}u_{i,N_y-5}), (i = 0, 1 \cdots, N_x). \tag{19}$$

According to the derivation, the truncation error of scheme (15) is $O(\tau^2 + h_x^4 + h_y^4)$. We notice that scheme (15) is a two-level scheme and the calculation of each unknown time level only involves five grid points. Since the right hand of the scheme (15) contains unknown items $(u_x)_{i,j}^{n+1}$ and $(u_y)_{i,j}^{n+1}$, so we use the successive over relaxation (SOR) method to iteratively solve it.

2.2. Stability Analysis

Now, we discuss the stability of the present HOC scheme by the von Neumann analysis method. To make it easier, in Equation (1), we assume that the coefficients of convection terms and reaction term are constants, which are $\bar{p}, \bar{q}$ and $\bar{c}$ ($\bar{c}$ is non-negative), respectively, then Equation (1) can be written as

$$u_t + \bar{p}u_x + \bar{q}u_y + \bar{c}u = \alpha(u_{xx} + u_{yy}) + f(x, y, t). \tag{20}$$

Then, assuming $f(x, y, t) \equiv 0$, we get the error equation of Equation (15)

$$\begin{aligned} &\delta_t^+ \varepsilon_{i,j}^n - \tau\alpha\delta_t^+\delta_x^2\varepsilon_{i,j}^n + \frac{\tau\alpha}{2}\delta_t^+\delta_x(\varepsilon_x)_{i,j}^n - \tau\alpha\delta_t^+\delta_y^2\varepsilon_{i,j}^n \\ &+ \frac{\tau\alpha}{2}\delta_t^+\delta_y(\varepsilon_y)_{i,j}^n + \frac{\tau}{2}\bar{p}\delta_t^+(\varepsilon_x)_{i,j}^n + \frac{\tau}{2}\bar{q}\delta_t^+(\varepsilon_y)_{i,j}^n + \frac{\tau}{2}\bar{c}\delta_t^+\varepsilon_{i,j}^n \\ &= 2\alpha\delta_x^2\varepsilon_{i,j}^n - \alpha\delta_x(\varepsilon_x)_{i,j}^n + 2\alpha\delta_y^2\varepsilon_{i,j}^n - \alpha\delta_y(\varepsilon_y)_{i,j}^n - \bar{p}(\varepsilon_x)_{i,j}^n - \bar{q}(\varepsilon_y)_{i,j}^n - \bar{c}\varepsilon_{i,j}^n. \end{aligned} \tag{21}$$

in which $\varepsilon_{i,j}^n$ represents the error generated by the numerical solution $u_{i,j}^n$. Use $(\varepsilon_x)_{i,j}^n$ and $(\varepsilon_y)_{i,j}^n$ to express the errors generated by the numerical solutions $(u_x)_{i,j}^n$ and $(u_y)_{i,j}^n$, respectively. At the grid node (x_i, y_j, t_n), let

$$\varepsilon_{i,j}^n = \xi^n e^{I\theta_x i} e^{I\theta_y j}, \tag{22}$$

$$(\varepsilon_x)_{i,j}^n = (\eta_x)^n e^{I\theta_x i} e^{I\theta_y j}, \tag{23}$$

$$(\varepsilon_y)_{i,j}^n = (\eta_y)^n e^{I\theta_x i} e^{I\theta_y j}, \tag{24}$$

where $I = \sqrt{-1}$, ξ^n, $(\eta_x)^n$, and $(\eta_y)^n$ are the amplitudes at the (n)th time level, while $\theta_x = \frac{2\pi h_x}{\lambda_1}$ and $\theta_y = \frac{2\pi h_y}{\lambda_2}$ are the phase angles in two spatial directions, respectively, in which λ_1 and λ_2 are the wavelengths, respectively. Substituting Equations (22)–(24) into Equation (21), and eliminating $e^{I\theta_x i} e^{I\theta_y j}$, we can get

$$
\begin{aligned}
&(\frac{1}{\tau}+\frac{2\alpha}{h_x^2}+\frac{2\alpha}{h_y^2}+\frac{\bar{c}}{2})\xi^{n+1}-\frac{\alpha}{h_x^2}(e^{I\theta_x}+e^{-I\theta_x})\xi^{n+1}-\frac{\alpha}{h_y^2}(e^{I\theta_y}+e^{-I\theta_y})\xi^{n+1}\\
&+\frac{\alpha}{4h_x}(e^{I\theta_x}-e^{-I\theta_x})(\eta_x)^{n+1}+\frac{\bar{p}}{2}(\eta_x)^{n+1}+\frac{\alpha}{4h_y}(e^{I\theta_y}-e^{-I\theta_y})(\eta_y)^{n+1}+\frac{\bar{q}}{2}(\eta_y)^{n+1}\\
&=(\frac{1}{\tau}-\frac{2\alpha}{h_x^2}-\frac{2\alpha}{h_y^2}-\frac{\bar{c}}{2})\xi^{n}+\frac{\alpha}{h_x^2}(e^{I\theta_x}+e^{-I\theta_x})\xi^{n}+\frac{\alpha}{h_y^2}(e^{I\theta_y}+e^{-I\theta_y})\xi^{n}\\
&-\frac{\alpha}{4h_x}(e^{I\theta_x}-e^{-I\theta_x})(\eta_x)^{n}-\frac{\bar{p}}{2}(\eta_x)^{n}-\frac{\alpha}{4h_y}(e^{I\theta_y}-e^{-I\theta_y})(\eta_y)^{n}-\frac{\bar{q}}{2}(\eta_y)^{n}.
\end{aligned}
\tag{25}
$$

According to Equations (6) and (7), we have

$$
(\eta_x)^n=\frac{3(e^{I\theta_x}-e^{-I\theta_x})}{h_x(e^{I\theta_x}+4+e^{-I\theta_x})}\xi^n, \tag{26}
$$

$$
(\eta_y)^n=\frac{3(e^{I\theta_y}-e^{-I\theta_y})}{h_y(e^{I\theta_y}+4+e^{-I\theta_y})}\xi^n. \tag{27}
$$

Substitute Equations (26) and (27) into Equation (25), then after simplification and rearrangement, we have

$$
\begin{aligned}
&\{1+\frac{\tau\bar{c}}{2}-2\tau\alpha(\frac{\cos\theta_x-1}{h_x^2}+\frac{\cos\theta_y-1}{h_y^2})-\frac{\tau\alpha}{2}[\frac{3\sin^2\theta_x}{h_x^2(2+\cos\theta_x)}+\frac{3\sin^2\theta_y}{h_y^2(2+\cos\theta_y)}]\\
&+\frac{3\tau}{2}[\frac{\bar{p}\sin\theta_x}{h_x(2+\cos\theta_x)}+\frac{\bar{q}\sin\theta_y}{h_y(2+\cos\theta_y)}]I\}\xi^{n+1}\\
&=\{1-\frac{\tau\bar{c}}{2}+2\tau\alpha(\frac{\cos\theta_x-1}{h_x^2}+\frac{\cos\theta_y-1}{h_y^2})+\frac{\tau\alpha}{2}[\frac{3\sin^2\theta_x}{h_x^2(2+\cos\theta_x)}+\frac{3\sin^2\theta_y}{h_y^2(2+\cos\theta_y)}]\\
&-\frac{3\tau}{2}[\frac{\bar{p}\sin\theta_x}{h_x(2+\cos\theta_x)}+\frac{\bar{q}\sin\theta_y}{h_y(2+\cos\theta_y)}]I\}\xi^{n}.
\end{aligned}
\tag{28}
$$

then the error amplification factor can be taken as

$$
G=\frac{\xi^{n+1}}{\xi^n}=\frac{1-A-BI}{1+A+BI}, \tag{29}
$$

where

$$
A=\frac{\tau\bar{c}}{2}-\frac{\tau\alpha}{2}[\frac{(\cos\theta_x-1)(\cos\theta_x+5)}{h_x^2(2+\cos\theta_x)}+\frac{(\cos\theta_y-1)(\cos\theta_y+5)}{h_y^2(2+\cos\theta_y)}], \tag{30}
$$

$$
B=\frac{3\tau}{2}[\frac{\bar{p}\sin\theta_x}{h_x(2+\cos\theta_x)}+\frac{\bar{q}\sin\theta_y}{h_y(2+\cos\theta_y)}]. \tag{31}
$$

From Equation (30), we find that $A\geq 0$, so $\|G\|^2=\frac{(1-A)^2+B^2}{(1+A)^2+B^2}\leq 1$. Therefore, we can conclude that the present HOC scheme Equation (15) is unconditionally stable.

3. Extension to 3D

Next, we pay attention to the 3D unsteady CDR equation with variable coefficients as follows:

$$
\begin{aligned}
&u_t+p(x,y,z,t)u_x+q(x,y,z,t)u_y+r(x,y,z,t)u_z+c(x,y,z,t)u\\
&=\alpha(u_{xx}+u_{yy}+u_{zz})+f(x,y,z,t),\ (x,y,z)\in\Omega, t\geq 0,
\end{aligned}
\tag{32}
$$

with initial condition

$$
u(x,y,z,0)=g(x,y,z),\ (x,y,z)\in\Omega, \tag{33}
$$

and boundary condition

$$u(x,y,z,t) = s(x,y,z,t),\ (x,y,z) \in \partial\Omega,\ t > 0. \tag{34}$$

where $\Omega = \{(x,y,z) : a_1 \le x \le b_1, a_2 \le y \le b_2, a_3 \le z \le b_3\}$, a_1, a_2, a_3, b_1, b_2, and b_3 are constants, $\partial\Omega$ is the boundary of Ω, α is the constant diffusion coefficient ($\alpha > 0$), $p(x,y,z,t)$, $q(x,y,z,t)$ and $r(x,y,z,t)$ are convection coefficients in the x-, y- , and z- directions, respectively, $c(x,y,z,t)$ is the reaction coefficient, and it is non-negative. p, q, r, c and exterior force f are regular enough and their required derivatives exist. We assume that $g(x,y,z)$ and $s(x,y,z,t)$ are known functions of sufficient smoothness and satisfy the compatibility condition $s(x,y,z,0) = g(x,y,z)$ for $(x,y,z) \in \partial\Omega$ such that the initial-boundary value problem (32)–(34) owns a unique solution.

In order to establish HOC difference scheme of model Equation (32), we divide the domain Ω into uniform mesh. In the x- direction: $a_1 = x_0, x_1, x_2, \cdots, x_{N_x} = b_1$, in the y-direction: $a_2 = y_0, y_1, y_2, \cdots, y_{N_y} = b_2$, in the z- direction: $a_3 = z_0, z_1, z_2, \cdots, z_{N_z} = b_3$, with the space step length $h_x = x_i - x_{i-1}$, $1 \le i \le N_x$, $h_y = y_j - y_{j-1}$, $1 \le j \le N_y$ and $h_z = z_k - z_{k-1}$, $1 \le k \le N_z$, τ represents the time step length, $t_n = n\tau, 0 \le n \le M$. The discretization of $u(x,y,z,t)$ at point (x_i, y_j, z_k, t_n) is expressed as $u^n_{i,j,k}$. Define the difference operators in three spatial directions as follows:

$$\delta_x u^n_{i,j,k} = \frac{u^n_{i+1,j,k} - u^n_{i-1,j,k}}{2h_x},\ \delta_x^2 u^n_{i,j,k} = \frac{u^n_{i+1,j,k} - 2u^n_{i,j,k} + u^n_{i-1,j,k}}{h_x^2}, \tag{35}$$

$$\delta_y u^n_{i,j,k} = \frac{u^n_{i,j+1,k} - u^n_{i,j-1,k}}{2h_y},\ \delta_y^2 u^n_{i,j,k} = \frac{u^n_{i,j+1,k} - 2u^n_{i,j,k} + u^n_{i,j-1,k}}{h_y^2}, \tag{36}$$

$$\delta_z u^n_{i,j,k} = \frac{u^n_{i,j,k+1} - u^n_{i,j,k-1}}{2h_z},\ \delta_z^2 u^n_{i,j,k} = \frac{u^n_{i,j,k+1} - 2u^n_{i,j,k} + u^n_{i,j,k-1}}{h_z^2}. \tag{37}$$

By a similar derivation, we can get the HOC difference scheme for the 3D unsteady CDR Equation (32) as following

$$\begin{aligned}
&\delta_t^+ u^n_{i,j,k} - \tau\alpha\delta_t^+\delta_x^2 u^n_{i,j,k} + \frac{\tau\alpha}{2}\delta_t^+\delta_x (u_x)^n_{i,j,k} - \tau\alpha\delta_t^+\delta_y^2 u^n_{i,j,k} + \frac{\tau\alpha}{2}\delta_t^+\delta_y (u_y)^n_{i,j,k} \\
&- \tau\alpha\delta_t^+\delta_z^2 u^n_{i,j,k} + \frac{\tau\alpha}{2}\delta_t^+\delta_z (u_z)^n_{i,j,k} + \frac{\tau}{2}\delta_t^+ p^n_{i,j,k}\cdot(u_x)^n_{i,j,k} + \frac{\tau}{2}p^n_{i,j,k}\delta_t^+(u_x)^n_{i,j,k} \\
&+ \frac{\tau}{2}\delta_t^+ q^n_{i,j,k}\cdot(u_y)^n_{i,j,k} + \frac{\tau}{2}q^n_{i,j,k}\delta_t^+(u_y)^n_{i,j,k} + \frac{\tau}{2}\delta_t^+ r^n_{i,j,k}\cdot(u_z)^n_{i,j,k} + \frac{\tau}{2}r^n_{i,j,k}\delta_t^+(u_z)^n_{i,j,k} \\
&+ \frac{\tau}{2}\delta_t^+ c^n_{i,j,k}\cdot u^n_{i,j,k} + \frac{\tau}{2}c^n_{i,j,k}\delta_t^+ u^n_{i,j,k} - \frac{\tau}{2}\delta_t^+ f^n_{i,j,k} \\
&= 2\alpha\delta_x^2 u^n_{i,j,k} - \alpha\delta_x (u_x)^n_{i,j,k} + 2\alpha\delta_y^2 u^n_{i,j,k} - \alpha\delta_y (u_y)^n_{i,j,k} + 2\alpha\delta_z^2 u^n_{i,j,k} - \alpha\delta_z (u_z)^n_{i,j,k} \\
&- p^n_{i,j,k}(u_x)^n_{i,j,k} - q^n_{i,j,k}(u_y)^n_{i,j,k} - r^n_{i,j,k}(u_z)^n_{i,j,k} - c^n_{i,j,k}u^n_{i,j,k} + f^n_{i,j,k}.
\end{aligned} \tag{38}$$

where δ_t^+ represents the forward difference operator of the first derivative in the time direction.

In Equation (38), u_x, u_y, and u_z are calculated by the fourth-order Padé difference formulas [40], while u_{xx}, u_{yy}, and u_{zz} are discretized by fourth-order compact difference formulas (see Appendix A). In addition, we adopt consistent fourth-order formulas [41] to calculate the values at the boundary points of u_x, u_y, and u_z (also see Appendix A).

Equation (38) is the HOC difference scheme for the 3D unsteady variable coefficients CDR equation. The calculation of each unknown time level only involves seven grid points. The truncation error is $O(\tau^2 + h_x^4 + h_y^4 + h_z^4)$. The right hand of the scheme (38) contains unknown items $(u_x)^{n+1}_{i,j,k}$, $(u_y)^{n+1}_{i,j,k}$ and $(u_z)^{n+1}_{i,j,k}$, so we use the SOR method to solve it. In addition, we should mention that the stability analysis of the 3D case is the same as that of the 2D case (see Appendix B). So, the scheme (38) is still unconditionally stable.

4. Numerical Experiments

Now, five examples are conducted to verify the effectiveness and validity of the new HOC difference schemes. We will compare the numerical results computed by the present HOC schemes with those derived by the methods in the existing literature. We note that for the methods in [42,43], we use PHOEBESolver software (http://www.phoebesolver.com/webpde/main/index) (accessed on 2 Feburary 2022) to calculate. For all calculations, an equal mesh size step is used in the spatial directions. We use the maximum absolute error L_∞ and the L_2 norm error to measure the accuracy of the new HOC schemes. The definitions of the two errors for 2D cases are:

$$L_\infty = \underset{i,j}{Max}\left|u_{i,j}^{exact} - u_{i,j}^{num}\right|, L_2 = \sqrt{h^2 \sum_i \sum_j \left(u_{i,j}^{exact} - u_{i,j}^{num}\right)^2},$$

and the definitions for 3D cases are:

$$L_\infty = \underset{i,j,k}{Max}\left|u_{i,j,k}^{exact} - u_{i,j,k}^{num}\right|, L_2 = \sqrt{h^3 \sum_i \sum_j \sum_k \left(u_{i,j,k}^{exact} - u_{i,j,k}^{num}\right)^2},$$

The definition of convergence rate is:

$$Rate = \frac{\log(E_1/E_2)}{\log(h_1/h_2)}.$$

in which E_1 and E_2 represent the errors corresponding to the different spatial step-lengths h_1 and h_2, respectively.

Problem 1. *Firstly, we pay attention to the 2D Burgers equation [42,44,45]:*

$$u_t + u(u_x + u_y) = \alpha(u_{xx} + u_{yy}), \quad (x, y) \in [0, 1]^2, t \in (0, T].$$

the initial and boundary conditions can be taken directly from the analytical solution $u(x, y, t) = 1/(1 + e^{\frac{x+y-t}{2\alpha}})$.

Problem 1 has nonlinear terms, which can still be approximated by the skill of solving linear problems in this study. In Table 1, the diffusion coefficient α is assigned to different values when $\tau = \frac{h^2}{\sqrt{15}\alpha}$, $T = \frac{1}{\sqrt{15}}$. We find that the scheme in Ref. [42] is fourth order in space, and the schemes in Ref. [44] are fourth and sixth order, respectively. We can see from the data that when $\alpha = 0.1$ in the present scheme, the fourth-order scheme in Ref. [44] and the scheme in Ref. [42] all achieve theoretical accuracy. At the same time, the sixth-order scheme in Ref. [44] obtains sixth-order accuracy. However, the L_∞ error calculated by the sixth-order scheme in Ref. [44] is larger than that in Ref. [42] and the present scheme. When $\alpha = 0.01$, the L_∞ error of the new scheme has the same order of magnitude as that of the scheme in Ref. [42], which is three to four orders lower than the fourth-order scheme in Ref. [44] and two orders lower than the sixth-order scheme in Ref. [44]. With the increase of mesh number, the present scheme makes the numerical approximation more accurate than Ref. [42]. When $N = 7, \tau = 0.01$ and $\alpha = 1$, the absolute error of different time is given in Table 2. It shows that the numerical results of the present scheme are six orders of magnitude lower than those in Ref. [45] and more accurate than those in Ref. [42]. The absolute errors when $h = 0.05, \tau = 0.001$ and $\alpha = 0.05$ of the present method and the HOC scheme in Ref. [42] are shown in Figure 1. By comparison, we can see that the absolute errors of the two schemes have the same order of magnitude when $T = 1$, while when $T = 2$, the absolute error of the present scheme is smaller. Figure 2 shows the numerical solutions of this problem for different times. We find that with the increase of time, the solution tends to a fixed value.

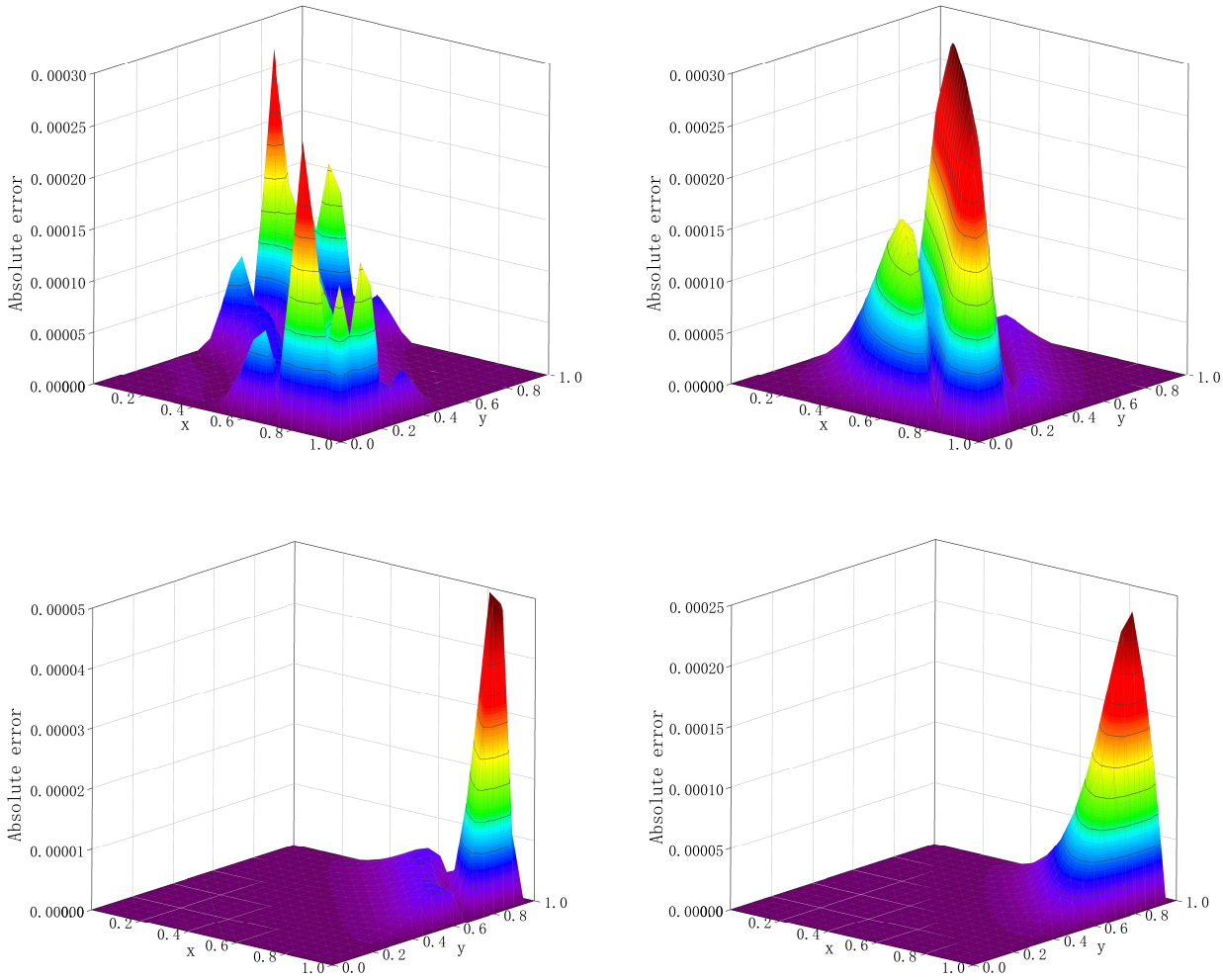

Figure 1. The absolute error when $h = 0.05, \tau = 0.001$ and $\alpha = 0.05$ for Problem 1. Top pictures: $T = 1$; under pictures: $T = 2$; left pictures: present scheme; right pictures: HOC scheme [42].

Table 1. The L_∞ error and convergence rate when $\tau = \frac{h^2}{\sqrt{15}\alpha}$, $T = \frac{1}{\sqrt{15}}$ for Problem 1.

		4-Order [44]		6-Order [44]		Ref. [42]		Present Scheme	
	h	L_∞	*Rate*	L_∞	*Rate*	L_∞	*Rate*	L_∞	*Rate*
$\alpha = 0.1$	1/20	4.099 (−3)		4.227 (−4)		1.209 (−5)		7.599 (−6)	
	1/40	4.031 (−4)	3.35	1.333 (−5)	4.99	7.552 (−7)	3.91	6.056 (−7)	3.65
	1/80	3.156 (−5)	3.67	2.948 (−7)	5.50	4.726 (−8)	4.00	4.002 (−8)	3.92
	1/160	2.207 (−6)	3.84	5.479 (−9)	5.75	2.954 (−9)	4.00	2.537 (−9)	3.98
$\alpha = 0.01$	1/40	–		–		2.954 (−2)		3.067 (−2)	
	1/80	–	–	–	–	1.732 (−3)	4.09	1.673 (−3)	4.20
	1/160	1.921 (−1)	–	2.937 (−2)	–	1.032 (−4)	4.07	1.019 (−4)	4.04
	1/320	1.854 (−2)	3.64	9.644 (−4)	4.93	6.370 (−6)	4.02	6.349 (−6)	4.00
	1/640	1.468 (−3)	3.37	2.236 (−5)	5.43	3.987 (−7)	4.00	3.972 (−7)	4.00

Table 2. The absolute error when $N = 7, \tau = 0.01, \alpha = 1$ for Problem 1.

x	y	$T = 15$			$T = 20$		
		Ref. [42]	**Ref. [45]**	**Present Scheme**	**Ref. [42]**	**Ref. [45]**	**Present Scheme**
1/7	1/7	2.513 (−11)	1.696 (−5)	9.053 (−12)	2.083 (−12)	1.395 (−6)	3.380 (−13)
3/7		5.018 (−11)	3.241 (−5)	2.104 (−11)	4.161 (−12)	2.667 (−6)	1.616 (−12)
5/7		5.041 (−11)	3.037 (−5)	1.926 (−11)	4.083 (−12)	2.499 (−6)	1.537 (−12)
1/7	3/7	5.072 (−11)	3.241 (−5)	2.104 (−11)	4.161 (−12)	2.667 (−6)	1.616 (−12)
3/7		1.076 (−10)	6.488 (−5)	4.623 (−11)	8.925 (−12)	5.340 (−6)	3.774 (−12)
5/7		1.059 (−10)	5.937 (−5)	4.147 (−11)	8.795 (−12)	4.883 (−6)	3.303 (−12)
1/7	5/7	5.041 (−11)	3.037 (−5)	1.926 (−11)	4.183 (−12)	2.499 (−6)	1.537 (−12)
3/7		1.059 (−10)	5.933 (−5)	4.147 (−11)	8.795 (−12)	4.883 (−6)	3.303 (−12)
5/7		1.041 (−10)	5.511 (−5)	3.717 (−11)	8.722 (−12)	4.573 (−6)	2.930 (−12)

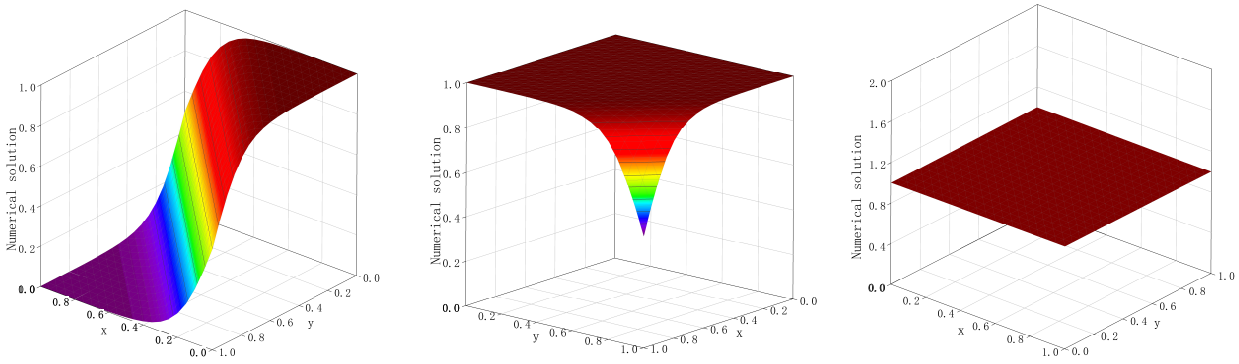

Figure 2. The numerical solution when $h = 0.05, \tau = 0.001$ and $\alpha = 0.05$ for problem 1. left: $T = 1$; middle: $T = 2$; right: $T = 4$.

Problem 2. *Next, we consider a 2D problem with exponential and characteristic boundary layers [12,20]:*

$$u_t + pu_x + qu_y = \alpha(u_{xx} + u_{yy}) + f(x, y, t), \quad (x, y) \in [0, 1]^2, t \in (0, T]$$

with $p = 1, q = 0, \alpha = 0.0001, f(x, y, t) = 1$. *Homogeneous Dirichlet boundary conditions are applied for this problem, and the initial condition is given as* $u(x, y, 0) = 0$.

The CDR equation consists of three parts: convection refers to the movement of molecules from one region to another because of velocity, while diffusion means the spread of particles through random motion from a region with high concentration to a low concentration region. Finally, reaction is due to the adsorption or chemical reaction of a substance with another component. For Problem 2, convection is dominated. While $q = 0$ means that the flow is only in the x-direction, thus forming an outflow boundary at $x = 1$. In fact, Problem 2 is an experiment with one exponential boundary layer and two characteristic boundary layers, which was studied in Refs. [12,20]. An exponential boundary layer appears at the outflow boundary $x = 1$. Meanwhile, $y = 0$ and $y = 1$ are the tangential boundaries, and characteristic or parabolic boundary layers develop there. There is no analytical solution for this problem. Take time step-length $\tau = 0.001$ and 120×120 grid nodes are used in the present scheme for numerical approximation. Figure 3 shows the numerical results of this problem at time $T = 0.3$, $T = 0.6$, $T = 0.9$, and $T = 1.2$. As time increases, this problem forms a slope in the calculation region from the entrance to the exit over time gradually. An adaptive mesh finite element method in Ref. [12] and an unstructured mesh difference method in Ref. [20] were used to carry out numerical simulation for this question, respectively, when $T = 0.6$ and $T = 1.2$. Comparing Figure 3b and Figure 3d with the figures in Refs. [12,20], it can be seen that both the present HOC

difference scheme and the above two schemes can accurately simulate this flow problem, which means that there is no numerical oscillation at the boundary layers.

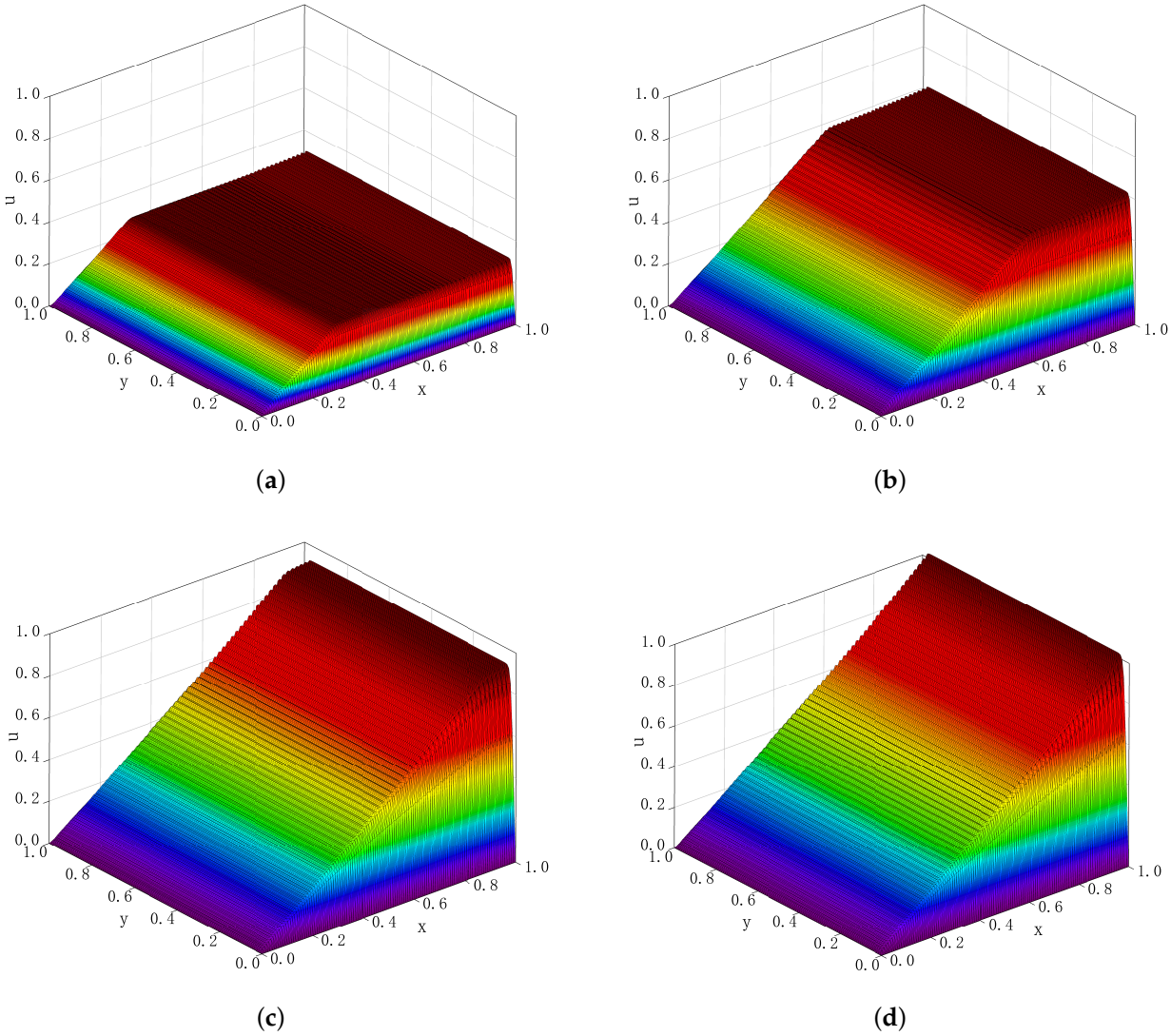

Figure 3. Numerical solutions of the present HOC scheme for Problem 2 when $h = \frac{1}{120}, \tau = 0.001$, (**a**) $T = 0.3$; (**b**) $T = 0.6$; (**c**) $T = 0.9$; (**d**) $T = 1.2$.

Problem 3. *Afterward, we consider the 2D inhomogeneous CDR equations:*

$$\begin{cases} u_t + \dfrac{a}{2}(u_x + u_y) = \dfrac{d}{2}(u_{xx} + u_{yy}) - bu + v \\ v_t + \dfrac{a}{2}(v_x + v_y) = \dfrac{d}{2}(v_{xx} + v_{yy}) - sv \end{cases} \quad (x, y) \in [0, 2\pi]^2, t \in (0, T].$$

This problem has the following analytical solution:

$$\begin{cases} u(x, y, t) = (e^{-(b+d)t} + e^{-(s+d)t}) \cos(x + y - at) \\ v(x, y, t) = (b - s)e^{-(s+d)t} \cos(x + y - at). \end{cases}$$

The initial and boundary conditions are taken by the analytical solution.

For Problem 3, three cases with different coefficients are considered respectively when $\tau = h^2, T = 1$, which are reaction dominance, convection dominance, and diffusion

dominance, accordingly. In Table 3, two norm errors and the convergence rates are shown when $a = d = s = 1, b = 100$. In this case, the governing equation is reaction dominated. We can see from the data that the convergence rates of variables u and v are both the fourth order in space. We notice that when the grid number takes 20, the calculation results are not very accurate; it is caused by too few grids or too few time advance steps. With the increase of grid number, the accuracy will be stabilized at the fourth order. The equation is convection dominated when $a = 1, b = 0.01, s = 0.1, d = 0.001$. Table 4 shows the errors and the convergence rate in this case. We can see that both the L_∞ and L_2 errors for u and v reach the fourth-order accuracy. When $a = s = 0.01, b = 0.1, d = 10$, the equation is diffusion dominated. In Table 5, we notice that the convergence rate of the two norm errors are still fourth order, which fully verifies the accuracy of the present scheme.

Table 3. The L_∞ error, L_2 error and convergence rate when $a = d = s = 1, b = 100$ for Problem 3.

h	u				v			
	L_∞	*Rate*	L_2	*Rate*	L_∞	*Rate*	L_2	*Rate*
1/20	2.096 (−2)		7.027 (−2)		1.240 (−1)		4.345 (−1)	
1/40	7.634 (−5)	8.10	2.665 (−4)	8.04	7.558 (−3)	4.04	2.638 (−2)	4.04
1/80	4.827 (−6)	3.98	1.687 (−5)	3.98	4.779 (−4)	3.98	1.670 (−3)	3.98
1/160	3.018 (−7)	4.00	1.054 (−6)	4.00	2.987 (−5)	4.00	1.043 (−5)	4.00

Table 4. The L_∞ error, L_2 error and convergence rate when $a = 1, b = 0.01, s = 0.1, d = 0.001$ for Problem 3.

h	u				v			
	L_∞	*Rate*	L_2	*Rate*	L_∞	*Rate*	L_2	*Rate*
1/20	1.728 (−3)		6.564 (−3)		7.351 (−5)		2.862 (−4)	
1/40	1.116 (−4)	3.95	4.283 (−4)	3.94	4.883 (−6)	3.91	1.866 (−5)	4.01
1/80	6.837 (−6)	4.03	2.167 (−5)	4.30	2.999 (−7)	4.03	1.163 (−6)	4.00
1/160	4.220 (−7)	4.02	1.673 (−6)	3.70	1.860 (−8)	4.01	7.293 (−8)	4.00

Table 5. The L_∞ error, L_2 error and convergence rate when $a = s = 0.01, b = 0.1, d = 10$ for Problem 3.

h	u				v			
	L_∞	*Rate*	L_2	*Rate*	L_∞	*Rate*	L_2	*Rate*
1/20	3.198 (−3)		9.985 (−3)		1.484 (−4)		4.633 (−4)	
1/40	1.879 (−4)	4.09	5.871 (−4)	4.09	8.726 (−6)	4.09	2.727 (−5)	4.09
1/80	1.213 (−5)	3.95	3.788 (−5)	3.95	5.629 (−7)	3.95	1.758 (−6)	3.96
1/160	7.571 (−7)	4.00	2.366 (−6)	4.00	3.515 (−8)	4.00	1.098 (−7)	4.00

Problem 4. *Now, we focus on a 3D CDR equation:*

$$u_t + t(x+y+z)u_x + t^2xyzu_y + \sin[\pi(x+y+z+t)]u_z + txyzu$$
$$= u_{xx} + u_{yy} + u_{zz} + f(x,y,z,t), \quad (x,y,z) \in [0,1]^3, t \in (0,T]$$

The analytical solution is $u(x,y,z,t) = e^t \sin(\pi x)\sin(\pi y)\sin(\pi z)$*, which gives the right hand term* $f(x,y,z,t)$ *and the initial and boundary conditions.*

Problem 4 is an inhomogeneous variable coefficient equation. When $\tau = h^2, T = 0.25$, the two norm errors and convergence rate of different space step-length are shown in Table 6. We find that the present scheme obtains fourth-order accuracy in space, while the C-N scheme and backward for time and central for space (BTCS) scheme only achieve second-order accuracy. When $T = 0.5, h = 0.03125$, the L_∞ error, L_2 error and convergence rate of different time step-length τ are shown in Table 7. From the numerical results, we

can get that the new HOC scheme obtains second-order accuracy in time. Table 8 displays the maximum absolute error L_∞ and L_2 error of different mesh ratios λ when $T = 1, h = \frac{1}{32}$. It is easy to see that the present scheme is still convergent when $\lambda > 1$ just like the C-N scheme and BTCS scheme. Therefore, the present HOC scheme for the 3D problem is unconditionally stable.

Table 6. The L_∞ error, L_2 error and convergence rate when $\tau = h^2, T = 0.25$ for Problem 4.

h	C-N Scheme				BTCS Scheme				Present Scheme			
	L_∞	*Rate*	L_2	*Rate*	L_∞	*Rate*	L_2	*Rate*	L_∞	*Rate*	L_2	*Rate*
1/8	1.58 (−2)		5.55 (−3)		1.62 (−2)		5.66 (−3)		2.83 (−4)		1.70 (−4)	
1/16	3.94 (−3)	2.00	1.38 (−3)	2.01	4.02 (−3)	2.01	1.41 (−3)	2.01	8.48 (−6)	5.06	4.10 (−6)	5.37
1/32	9.83 (−4)	2.00	3.44 (−4)	2.00	1.00 (−3)	2.01	3.52 (−4)	2.00	4.30 (−7)	4.30	1.76 (−7)	4.54
1/64	2.46 (−4)	2.00	8.61 (−5)	2.00	2.51 (−4)	1.99	8.79 (−5)	2.00	2.52 (−8)	4.09	9.75 (−9)	4.17

Table 7. The L_∞ error, L_2 error and convergence rate when $h = 0.03125, T = 0.5$ for Problem 4.

τ	L_∞	*Rate*	L_2	*Rate*
0.1	8.220 (−4)		2.528 (−4)	
0.05	2.017 (−4)	2.03	6.189 (−5)	2.03
0.025	5.056 (−5)	2.00	1.550 (−5)	2.00
0.0125	1.292 (−5)	1.97	3.920 (−6)	1.98
0.00625	3.519 (−6)	1.88	1.039 (−6)	1.92

Table 8. The L_∞ error and L_2 error when $h = \frac{1}{32}, T = 1$ with different mesh ratio $\lambda = \frac{\tau}{h^2}$ for Problem 4.

λ	Steps in the Time Direction	C-N Scheme		BTCS Scheme		Present Scheme	
		L_∞	L_2	L_∞	L_2	L_∞	L_2
0.8	1280	2.110 (−3)	7.362 (−4)	2.144 (−3)	7.458 (−4)	7.827 (−7)	3.002 (−7)
1.6	640	2.110 (−3)	7.362 (−4)	2.178 (−3)	7.608 (−4)	7.906 (−7)	2.496 (−7)
3.2	320	2.110 (−3)	7.364 (−4)	2.246 (−3)	7.854 (−4)	1.381 (−6)	4.394 (−7)
6.4	160	2.112 (−3)	7.371 (−4)	2.383 (−3)	8.345 (−4)	6.839 (−6)	2.142 (−6)

Problem 5. *Finally, we solve a 3D Burgers equation [43]:*

$$u_t + uu_x + vu_y + wu_z = \alpha(u_{xx} + u_{yy} + u_{zz}), \quad (x, y, z) \in [0, 1]^3, t \in (0, T]$$

in which

$$v(x, y, z, t) = -2\alpha[a_2 e^{-\gamma\alpha t} n_y \pi \sin(n_x \pi x) \cos(n_y \pi y) \sin(n_z \pi z)] d_0$$
$$w(x, y, z, t) = -2\alpha[a_2 e^{-\gamma\alpha t} n_z \pi \sin(n_x \pi x) \sin(n_y \pi y) \cos(n_z \pi z)] d_0.$$

and $\gamma = \pi^2(n_x^2 + n_y^2 + n_z^2)$, $d_0 = 1/[a_1 + a_2 e^{-\gamma\alpha t} \sin(n_x \pi x) \sin(n_y \pi y) \sin(n_z \pi z)]$ *are two parameters. The initial and boundary conditions can be taken from the analytical solution* $u(x, y, z, t) = -2\alpha[a_2 e^{-\gamma\alpha t} n_x \pi \cos(n_x \pi x) \sin(n_y \pi y) \sin(n_z \pi z)] d_0$.

Problem 5 is a 3D nonlinear convection diffusion case. We take $n_x = n_y = n_z = 3$, $a_1 = 1, a_2 = 0.1$ in the calculation. Table 9 shows the L_∞ error and convergence rate of the new scheme and the DHOC scheme [43] with different spatial grid numbers. The DHOC scheme is conditionally stable with the truncation error $O(\tau^2 + h_x^4 + h_y^4 + h_z^4)$. We find that both the two schemes obtain fourth-order accuracy in space when $\tau = h^2$. Table 10 shows the comparison of the maximum absolute error when $\tau = 0.001, T = 0.1$ with different α. We can see that the L_∞ error of the new HOC scheme has the same order of magnitude as that of the DHOC scheme, but the numerical results of the present scheme are more

accurate. Table 11 displays the L_∞ error and the L_2 error of different mesh ratio λ when $h = 0.0625, \alpha$=0.1, $T = 2$. With the increase of λ, the present scheme is still convergent, that is, unconditionally stable, while the DHOC scheme is divergent, that is, conditionally stable, which is consistent with the theoretical analysis and fully verifies the robustness of the new scheme.

Table 9. The L_∞ error and convergence rate when $\tau = h^2, \alpha = 0.1, T = 0.5$ for Problem 5.

h	*DHOC* [43]		Present Scheme	
	L_∞	L_2	L_∞	L_2
1/8	9.079 (−5)		5.848 (−5)	
1/16	2.555 (−6)	5.15	8.617 (−7)	6.08
1/32	2.267 (−8)	6.82	4.164 (−8)	4.37

Table 10. The L_∞ error when $\tau = 0.001, T = 0.1$ with different α for Problem 5.

α	$h = 0.1$		$h = 0.0625$	
	DHOC [43]	Present Scheme	*DHOC* [43]	Present Scheme
10^{-1}	4.764 (−4)	6.692 (−4)	7.195 (−5)	1.070 (−4)
10^{-2}	1.264 (−4)	1.195 (−4)	3.955 (−5)	2.632 (−5)
10^{-3}	1.914 (−6)	1.875 (−6)	6.366 (−7)	4.645 (−7)
10^{-4}	1.996 (−8)	1.963 (−8)	6.670 (−9)	4.937 (−9)
10^{-5}	2.004 (−10)	1.972 (−10)	6.701 (−11)	4.967 (−11)
10^{-6}	2.005 (−12)	1.973 (−12)	6.704 (−13)	4.970 (−13)

Table 11. The L_∞ error and L_2 error when $h = \frac{1}{16}, \alpha = 0.1, T = 2$ for different mesh ratio $\lambda = \frac{\tau}{h^2}$ for Problem 5.

λ	*DHOC* [43]		Present Scheme	
	L_∞	L_2	L_∞	L_2
1	4.782 (−10)	1.400 (−10)	7.213 (−10)	2.469 (−10)
2	5.190 (−10)	1.519 (−10)	7.231 (−10)	2.477 (−10)
4	4.547 (−7)	1.143 (−7)	7.255 (−10)	2.490 (−10)
6	1.212 (+0)	2.945 (−1)	7.468 (−10)	2.567 (−10)
8	1.093 (+1)	2.322 (+0)	7.326 (−10)	2.529 (−10)

5. Conclusions

In this study, an HOC method is introduced, and two HOC difference schemes are formulated to solve 2D and 3D unsteady CDR equations with variable coefficients. They have second-order temporal accuracy and fourth-order spatial accuracy. The stability of these two schemes are proven by using the von Neumann linear stability analysis method. For solving the linear algebraic systems generated by the HOC difference schemes at each time level, the SOR method is used. Numerical studies are carried out to validate the effectiveness and dependability of the novel schemes. We can see that the proposed schemes have high accuracy and very good stability. In addition, the present schemes have several obvious advantages as follows:

(1) The present difference scheme for the 2D case involves only five grid points, while the scheme in Ref. [32] has a nine-point stencil. Similarly, our scheme for the 3D case involves only seven grid points, while that in Ref. [24] has a 19-point stencil and those in Refs. [38,39] have 27-point stencils. So, the present HOC schemes make it easy to program and save storage space.

(2) Although the equation models are used to describe linear problems, the present schemes are also suitable for solving the Burgers equations with nonlinear terms and produce more accurate numerical results than those in the literature.

(3) The present schemes are unconditionally stable, which is uncommon for many HOC schemes for solving variable coefficients problems, especially for 3D cases. As we mentioned earlier, the methods in Refs. [36–39] are only suitable for solving 3D constant coefficients problems; at the same time, the method in Ref. [36] is conditionally stable.

As we know, chemotaxis models in biomathematics can be described by unsteady nonlinear convection diffusion reaction equations. Some researchers have used the finite difference method to study chemotaxis models. For instance, Chertock et al. [46] formulated a high-order finite volume-finite difference scheme for solving the Patlak–Keller–Segel chemotaxis model. The scheme has fourth-order accuracy but is conditionally stable. Later, Chertock et al. [47] generalized this method and proposed an adaptive mesh algorithm to simulate the blow-up phenomena of the chemotaxis model. Up to now, there have been few HOC difference methods to solve chemotaxis models. Although the present method cannot solve the complete nonlinear problems, we are planning to extend it to the fully nonlinear CDR equation and to solve chemotaxis models in our future work.

Author Contributions: J.W., methodology, software, validation, writing; Y.G., conceptualization, Funding acquisition, supervision; Y.W., Investigation, project administration. All authors have read and agreed to the published version of the manuscript.

Funding: This work is partially supported by the National Natural Science Foundation of China (12161067, 11961054, 11902170), the Key Research and Development Program of Ningxia (2018BEE03007), National Youth Top-notch Talent Support Program of Ningxia, and the First Class Discipline Construction Project in Ningxia Universities: Mathematics.

Institutional Review Board Statement: Not applicable.

Informed Consent Statement: Not applicable.

Data Availability Statement: Not applicable.

Conflicts of Interest: The authors declare no conflict of interest.

Appendix A

The first-derivative terms in the spatial direction in Equation (38) are calculated by the following fourth-order Padé approximation [40]

$$\frac{1}{6}(u_x)_{i-1,j,k}+\frac{2}{3}(u_x)_{i,j,k}+\frac{1}{6}(u_x)_{i+1,j,k}=\frac{u_{i+1,j,k}-u_{i-1,j,k}}{2h_x}+O(h_x^4), \tag{A1}$$

$$\frac{1}{6}(u_y)_{i,j-1,k}+\frac{2}{3}(u_y)_{i,j,k}+\frac{1}{6}(u_y)_{i,j+1,k}=\frac{u_{i,j+1,k}-u_{i,j-1,k}}{2h_y}+O(h_y^4), \tag{A2}$$

$$\frac{1}{6}(u_z)_{i,j,k-1}+\frac{2}{3}(u_z)_{i,j,k}+\frac{1}{6}(u_z)_{i,j,k+1}=\frac{u_{i,j,k+1}-u_{i,j,k-1}}{2h_z}+O(h_z^4). \tag{A3}$$

The second-derivative terms in Equation (38) are calculated by the following fourth-order compact formulas

$$(u_{dd})^n_{i,j,k}=2\delta_d^2u^n_{i,j,k}-\delta_d(u_d)^n_{i,j,k}+O(h_d^4), \tag{A4}$$

in which d presents x, y, and z. The boundaries of the first derivatives in Equation (38) are calculated by the following consistent fourth-order scheme [41]

$$\begin{aligned}(u_x)_{0,j,k}+\frac{14}{15}(u_x)_{1,j,k}=\frac{1}{h_x}(&-\frac{184}{75}u_{0,j,k}+\frac{703}{180}u_{1,j,k}-\frac{89}{30}u_{2,j,k}+\frac{67}{30}u_{3,j,k}\\&-\frac{77}{90}u_{4,j,k}+\frac{41}{300}u_{5,j,k})(j=0,1\cdots,N_y;k=0,1\cdots,N_z),\end{aligned} \tag{A5}$$

$$(u_y)_{i,0,k} + \frac{14}{15}(u_y)_{i,1,k} = \frac{1}{h_y}(-\frac{184}{75}u_{i,0,k} + \frac{703}{180}u_{i,1,k} - \frac{89}{30}u_{i,2,k} + \frac{67}{30}u_{i,3,k} - \frac{77}{90}u_{i,4,k} + \frac{41}{300}u_{i,5,k})(i = 0, 1, \cdots, N_x; k = 0, 1, \cdots, N_z), \tag{A6}$$

$$(u_z)_{i,j,0} + \frac{14}{15}(u_z)_{i,j,1} = \frac{1}{h_z}(-\frac{184}{75}u_{i,j,0} + \frac{703}{180}u_{i,j,1} - \frac{89}{30}u_{i,j,2} + \frac{67}{30}u_{i,j,3} - \frac{77}{90}u_{i,j,4} + \frac{41}{300}u_{i,j,5})(i = 0, 1 \cdots, N_x; j = 0, 1 \cdots, N_y), \tag{A7}$$

$$(u_x)_{N_x,j,k} - \frac{14}{15}(u_x)_{N_x-1,j,k} = \frac{1}{h_x}(\frac{52}{25}u_{N_x,j,k} - \frac{1067}{180}u_{N_x-1,j,k} + \frac{67}{10}u_{N_x-2,j,k} - \frac{41}{10}u_{N_x-3,j,k} + \frac{133}{90}u_{N_x-4,j,k} - \frac{69}{300}u_{N_x-5,j,k})(j = 0, 1 \cdots, N_y; k = 0, 1 \cdots, N_z), \tag{A8}$$

$$(u_y)_{i,N_y,k} - \frac{14}{15}(u_y)_{i,N_y-1,k} = \frac{1}{h_y}(\frac{52}{25}u_{i,N_y,k} - \frac{1067}{180}u_{i,N_y-1,k} + \frac{67}{10}u_{i,N_y-2,k} - \frac{41}{10}u_{i,N_y-3,k} + \frac{133}{90}u_{i,N_y-4,k} - \frac{69}{300}u_{i,N_y-5,k}),\ (i = 0, 1 \cdots, N_x; k = 0, 1 \cdots, N_z), \tag{A9}$$

$$(u_z)_{i,j,N_z} - \frac{14}{15}(u_z)_{i,j,N_z-1} = \frac{1}{h_z}(\frac{52}{25}u_{i,j,N_z} - \frac{1067}{180}u_{i,j,N_z-1} + \frac{67}{10}u_{i,j,N_z-2} - \frac{41}{10}u_{i,j,N_z-3} + \frac{133}{90}u_{i,j,N_z-4} - \frac{69}{300}u_{i,j,N_z-5}),\ (i = 0, 1 \cdots, N_x; j = 0, 1 \cdots, N_y). \tag{A10}$$

Appendix B

In Equation (32), we assume that the convection coefficients and reaction coefficient are constants, which are $\bar{p}, \bar{q}, \bar{r}$ and $\bar{c}$ ($\bar{c}$ is non-negative), respectively. At the same time, assuming $f(x, y, z, t) \equiv 0$, we obtain the error equation of Equation (38)

$$\begin{aligned}
&\delta_t^+\varepsilon_{i,j,k}^n - \tau\alpha\delta_t^+\delta_x^2\varepsilon_{i,j,k}^n + \frac{\tau\alpha}{2}\delta_t^+\delta_x(\varepsilon_x)_{i,j,k}^n - \tau\alpha\delta_t^+\delta_y^2\varepsilon_{i,j,k}^n + \frac{\tau\alpha}{2}\delta_t^+\delta_y(\varepsilon_y)_{i,j,k}^n - \tau\alpha\delta_t^+\delta_z^2\varepsilon_{i,j,k}^n \\
&+ \frac{\tau\alpha}{2}\delta_t^+\delta_z(\varepsilon_z)_{i,j,k}^n + \frac{\tau}{2}\bar{p}\delta_t^+(\varepsilon_x)_{i,j,k}^n + \frac{\tau}{2}\bar{q}\delta_t^+(\varepsilon_y)_{i,j,k}^n + \frac{\tau}{2}\bar{r}\delta_t^+(\varepsilon_z)_{i,j,k}^n + \frac{\tau}{2}\bar{c}\delta_t^+\varepsilon_{i,j,k}^n \\
&= 2\alpha\delta_x^2\varepsilon_{i,j,k}^n - \alpha\delta_x(\varepsilon_x)_{i,j,k}^n + 2\alpha\delta_y^2\varepsilon_{i,j,k}^n - \alpha\delta_y(\varepsilon_y)_{i,j,k}^n + 2\alpha\delta_z^2\varepsilon_{i,j,k}^n - \alpha\delta_z(\varepsilon_z)_{i,j,k}^n \\
&- \bar{p}(\varepsilon_x)_{i,j,k}^n - \bar{q}(\varepsilon_y)_{i,j,k}^n - \bar{r}(\varepsilon_z)_{i,j,k}^n - \bar{c}\varepsilon_{i,j,k}^n.
\end{aligned} \tag{A11}$$

in which $\varepsilon_{i,j,k}^n$ represents the error generated by the numerical solution $u_{i,j,k}^n$. Use $(\varepsilon_x)_{i,j,k}^n$, $(\varepsilon_y)_{i,j,k}^n$ and $(\varepsilon_z)_{i,j,k}^n$ to express the errors generated by the numerical solution $(u_x)_{i,j,k}^n$, $(u_y)_{i,j,k}^n$ and $(u_z)_{i,j,k}^n$, respectively.

At the grid (x_i, y_j, z_k, t_n) node , let

$$\varepsilon_{i,j,k}^n = \xi^n e^{I\theta_x i} e^{I\theta_y j} e^{I\theta_z k}, \tag{A12}$$

$$(\varepsilon_x)_{i,j,k}^n = (\eta_x)^n e^{I\theta_x i} e^{I\theta_y j} e^{I\theta_z k}, (\varepsilon_y)_{i,j,k}^n = (\eta_y)^n e^{I\theta_x i} e^{I\theta_y j} e^{I\theta_z k}, (\varepsilon_z)_{i,j,k}^n = (\eta_z)^n e^{I\theta_x i} e^{I\theta_y j} e^{I\theta_z k}. \tag{A13}$$

where $I = \sqrt{-1}$, ξ^n,$(\eta_x)^n$,$(\eta_y)^n$ and $(\eta_z)^n$ are the amplitudes at the (n)th time level, and $\theta_x = \frac{2\pi h_x}{\lambda_1}$, $\theta_y = \frac{2\pi h_y}{\lambda_2}$ and $\theta_z = \frac{2\pi h_z}{\lambda_3}$ are the phase angles in three spatial directions, respectively, in which λ_1, λ_2 and λ_3 represent the wavelengths.

Substituting Equations (A12) and (A13) into Equation (A11), and eliminating $e^{I\theta_x i}e^{I\theta_y j}e^{I\theta_z k}$ on both sides of the equation, we can get

$$\begin{aligned}
&(\frac{1}{\tau}+\frac{2\alpha}{h_x^2}+\frac{2\alpha}{h_y^2}+\frac{2\alpha}{h_z^2}+\frac{\bar{c}}{2})\xi^{n+1}-\frac{\alpha}{h_x^2}(e^{I\theta_x}+e^{-I\theta_x})\xi^{n+1}-\frac{\alpha}{h_y^2}(e^{I\theta_y}+e^{-I\theta_y})\xi^{n+1}\\
&-\frac{\alpha}{h_z^2}(e^{I\theta_z}+e^{-I\theta_z})\xi^{n+1}+\frac{\alpha}{4h_x}(e^{I\theta_x}-e^{-I\theta_x}){\eta_x}^{n+1}+\frac{\bar{p}}{2}{\eta_x}^{n+1}\\
&+\frac{\alpha}{4h_y}(e^{I\theta_y}-e^{-I\theta_y}){\eta_y}^{n+1}+\frac{\bar{q}}{2}{\eta_y}^{n+1}+\frac{\alpha}{4h_z}(e^{I\theta_z}-e^{-I\theta_z}){\eta_z}^{n+1}+\frac{\bar{r}}{2}{\eta_z}^{n+1}\\
&=(\frac{1}{\tau}-\frac{2\alpha}{h_x^2}-\frac{2\alpha}{h_y^2}-\frac{2\alpha}{h_z^2}-\frac{\bar{c}}{2})\xi^{n}+\frac{\alpha}{h_x^2}(e^{I\theta_x}+e^{-I\theta_x})\xi^{n}+\frac{\alpha}{h_y^2}(e^{I\theta_y}+e^{-I\theta_y})\xi^{n}\\
&+\frac{\alpha}{h_z^2}(e^{I\theta_z}+e^{-I\theta_z})\xi^{n}-\frac{\alpha}{4h_x}(e^{I\theta_x}-e^{-I\theta_x}){\eta_x}^{n}-\frac{\bar{p}}{2}{\eta_x}^{n}\\
&-\frac{\alpha}{4h_y}(e^{I\theta_y}-e^{-I\theta_y}){\eta_y}^{n}-\frac{\bar{q}}{2}{\eta_y}^{n}-\frac{\alpha}{4h_z}(e^{I\theta_z}-e^{-I\theta_z}){\eta_z}^{n}-\frac{\bar{r}}{2}{\eta_z}^{n}.
\end{aligned}\tag{A14}$$

According to Equations (A1)–(A3), we have

$$(\eta_x)^n=\frac{3(e^{I\theta_x}-e^{-I\theta_x})}{h_x(e^{I\theta_x}+4+e^{-I\theta_x})}\xi^n,\tag{A15}$$

$$(\eta_y)^n=\frac{3(e^{I\theta_y}-e^{-I\theta_y})}{h_y(e^{I\theta_y}+4+e^{-I\theta_y})}\xi^n,\tag{A16}$$

$$(\eta_z)^n=\frac{3(e^{I\theta_z}-e^{-I\theta_z})}{h_z(e^{I\theta_z}+4+e^{-I\theta_z})}\xi^n.\tag{A17}$$

Substituting Equations (A15)–(A17) into Equation (A14), then, after simplification and rearrangement, we have

$$\begin{aligned}
&\{1+\frac{\tau\bar{c}}{2}-2\tau\alpha(\frac{\cos\theta_x-1}{h_x^2}+\frac{\cos\theta_y-1}{h_y^2}+\frac{\cos\theta_z-1}{h_z^2})-\frac{\tau\alpha}{2}[\frac{3\sin^2\theta_x}{h_x^2(2+\cos\theta_x)}+\frac{3\sin^2\theta_y}{h_y^2(2+\cos\theta_y)}\\
&+\frac{3\sin^2\theta_z}{h_z^2(2+\cos\theta_z)}]+\frac{3\tau}{2}[\frac{\bar{p}\sin\theta_x}{h_x(2+\cos\theta_x)}+\frac{\bar{q}\sin\theta_y}{h_y(2+\cos\theta_y)}+\frac{\bar{r}\sin\theta_z}{h_z(2+\cos\theta_z)}]I\}\xi^{n+1}\\
&=\{1-\frac{\tau\bar{c}}{2}+2\tau\alpha(\frac{\cos\theta_x-1}{h_x^2}+\frac{\cos\theta_y-1}{h_y^2}+\frac{\cos\theta_z-1}{h_z^2})\\
&+\frac{\tau\alpha}{2}[\frac{3\sin^2\theta_x}{h_x^2(2+\cos\theta_x)}+\frac{3\sin^2\theta_y}{h_y^2(2+\cos\theta_y)}+\frac{3\sin^2\theta_z}{h_z^2(2+\cos\theta_z)}]\\
&-\frac{3\tau}{2}[\frac{\bar{p}\sin\theta_x}{h_x(2+\cos\theta_x)}+\frac{\bar{q}\sin\theta_y}{h_y(2+\cos\theta_y)}+\frac{\bar{r}\sin\theta_z}{h_z(2+\cos\theta_z)}]I\}\xi^n.
\end{aligned}\tag{A18}$$

The amplification factor is taken to be

$$G=\frac{\xi^{n+1}}{\xi^n}=\frac{1-A-BI}{1+A+BI},\tag{A19}$$

where

$$A=\frac{\tau\bar{c}}{2}-\frac{\tau\alpha}{2}[\frac{(\cos\theta_x-1)(\cos\theta_x+5)}{h_x^2(2+\cos\theta_x)}+\frac{(\cos\theta_y-1)(\cos\theta_y+5)}{h_y^2(2+\cos\theta_y)}+\frac{(\cos\theta_z-1)(\cos\theta_z+5)}{h_z^2(2+\cos\theta_z)}],\tag{A20}$$

$$B=\frac{3\tau}{2}[\frac{\bar{p}\sin\theta_x}{h_x(2+\cos\theta_x)}+\frac{\bar{q}\sin\theta_y}{h_y(2+\cos\theta_y)}+\frac{\bar{r}\sin\theta_z}{h_z(2+\cos\theta_z)}].\tag{A21}$$

From Equation (A20), we find that $A \geq 0$, so $\|G\|^2 = \frac{(1-A)^2+B^2}{(1+A)^2+B^2} \leq 1$. Therefore, we conclude that the present HOC Formula (38) is unconditionally stable.

References

1. Li, J.W.; Feng, X.L.; He, Y.N. RBF-based meshless local Petrov Galerkin method for the multi-dimensional convection-diffusion-reaction equation. *Eng. Anal. Bound. Elem.* **2019**, *98*, 46–53. [CrossRef]
2. Fu, Z.J.; Tang, Z.C.; Zhao, H.T.; Li, P.W.; Rabczuk, T. Numerical solutions of the coupled unsteady nonlinear convection-diffusion equations based on generalized finite difference method. *Eur. Phys. J. Plus* **2019**, *134*, 272. [CrossRef]
3. Sheshachala, S.K.; Codina, R. Finite element modeling of nonlinear reaction-diffusion-advection systems of equation. *Int. J. Numer. Methods Heat Fluid Flow* **2018**, *280*, 2688–2715. [CrossRef]
4. Li, L.Y.; Jiang, Z.W.; Yin, Z. Fourth-order compact finite difference method for solving two-dimensional convection-diffusion equation. *Adv. Differ. Equ.* **2018**, *234*, 234. [CrossRef]
5. Isenberg, J.; Gutfinger, C. Heat transfer to a draining film. *Int. J. Heat Mass Transf.* **1973**, *16*, 505–512. [CrossRef]
6. Brkié, D.; Stajié, Z. Excel VBA-based user defined functions for highly precise Colebrook's pipe flow friction approximations: a comparative overview. *Facta Univ. Ser. Mech. Eng.* **2021**, *19*, 253–269. [CrossRef]
7. Feijó, B.C.; Pavlovic, A.; Rocha, L.A.O.; Isoldi, L.A.; Lorente, S.; dos Santos, E.D. Geometrical investigation of microchannel with two trapezoidal blocks subjected to laminar convective flows with and without boiling. *Rep. Mech. Eng.* **2022**, *3*, 20–36. [CrossRef]
8. Noguez, M.A.; Botello, S.; Herrera, R.; Esqueda, H. Discretization of the 2D convection-diffusion equation using discrete exterior calculus. *J. Appl. Comput. Mech.* **2020**, *6*, 1348–1363.
9. Codina, R. Comparison of some finite element methods for solving the diffusion convection reaction equation. *Comput. Methods Appl. Mech. Eng.* **1998**, *156*, 185–210. [CrossRef]
10. Sinha, R.K.; Geiser, J. Error estimates for finite volume element methods for convection diffusion reaction equations. *Appl. Numer. Math.* **2007**, *57*, 59–72. [CrossRef]
11. John, V.; Schmeyer, E. Finite element methods for time dependent convection diffusion reaction equations with small diffusion. *Comput. Methods Appl. Mech. Eng.* **2008**, *198*, 475–494. [CrossRef]
12. de Frutos, J.; García-Archilla, B.; John, V.; Novo, J. An adaptive SUPG method for evolutionary convection-diffusion equations. *Comput. Methods Appl. Mech. Eng.* **2014**, *273*, 219–237. [CrossRef]
13. Sun, T. A second order characteristic mixed finite element method for convection diffusion reaction equations. *J. Appl. Math. Phys.* **2017**, *5*, 1301–1319. [CrossRef]
14. Qian, L.; Cai, H.; Guo, R.; Feng, X. The characteristic variational multiscale method for convection-dominated convection-diffusion-reaction problems. *Int. J. Heat Mass Transf.* **2014**, *72*, 461–469. [CrossRef]
15. Nie, Q.; Wan, F.; Zhang, Y.T.; Liu, X.F. Compact integration factor methods in high spatial dimensions. *J. Comput. Phys.* **2008**, *227*, 5238–5255. [CrossRef]
16. Zhao, S.; Ovadia, J.; Liu, X.F.; Zhang, Y.T.; Nie, Q. Operator splitting implicit integration factor methods for stiff reaction-diffusion-advection systems. *J. Comput. Phys.* **2011**, *230*, 5996–6009. [CrossRef]
17. Jiang, T.; Zhang, Y.T. Krylov single-step implicit integration factor WENO methods for advection diffusion reaction equations. *J. Comput. Phys.* **2016**, *311*, 22–44. [CrossRef]
18. Wei, T.; Xu, M. An integral equation approach to the unsteady convection-diffusion equations. *Appl. Math. Comput.* **2016**, *274*, 55–64. [CrossRef]
19. Lin, J.; Reutskiy, S.Y. An accurate meshless formulation for the simulation of linear and fully nonlinear advection diffusion reaction problems. *Adv. Eng. Softw.* **2018**, *126*, 127–146. [CrossRef]
20. Kaya, A. Finite difference approximations of multidimensional unsteady convection diffusion reaction equations. *J. Comput. Phys.* **2015**, *285*, 331–349. [CrossRef]
21. Hsieh, P.W.; Yang, S.Y.; You, C.S. A high-accuracy finite difference scheme for solving reaction-convection-diffusion problems with a small diffusivity. *Adv. Appl. Math. Mech.* **2014**, *6*, 637–662. [CrossRef]
22. Tong, F.H.; Feng, X.L.; Li, Z.L. Fourth order compact FD methods for convection diffusion equations with variable coefficients. *Appl. Math. Lett.* **2021**, *121*, 107413. [CrossRef]
23. Jha, N.; Singh, B. Exponential basis and exponential expanding grids third (fourth)-order compact schemes for nonlinear three-dimensional convection-diffusion-reaction equation. *Adv. Differ. Equ.* **2019**, *339*, 1–27. [CrossRef]
24. Ma, T.; Ge, Y. High-order blended compact difference schemes for the 3D elliptic partial equation with mixed derivatives and variable coefficients. *Adv. Differ. Equ.* **2020**, *2020*, 525. [CrossRef]
25. Biazar, J.; Mehrlatifan, M.B. A compact finite difference scheme for reaction convection diffusion equation. *Chiang Mai J. Sci.* **2018**, *45*, 1559–1568.
26. Liao, W. A compact high-order finite difference method for unsteady convection diffusion equation. *Int. J. Comput. Methods Eng. Sci. Mech.* **2012**, *13*, 135–145. [CrossRef]
27. Zhu, X.; Rui, H. High-order compact difference scheme of 1D nonlinear degenerate convection-reaction-diffusion equation with adaptive algorithm. *Numer. Heat Transf. Part B Fundam.* **2019**, *75*, 43–66. [CrossRef]
28. Karaa, S. An accurate LOD scheme for two-dimensional parabolic problems. *Appl. Math. Comput.* **2005**, *170*, 886–894. [CrossRef]

29. Courant, R.; Isaacson, E.; Rees, M. On the solution of nonlinear hyperbolic differential equations by finite differences. *Commun. Pure Appl. Math.* **1952**, *5*, 243–255. [CrossRef]
30. Noye, B.J.; Tan, H.H. A third-order semi-implicit finite difference method for solving the one-dimensional convection-diffusion equation. *Int. J. Numer. Methods Eng.* **1988**, *26*, 1615–1629. [CrossRef]
31. Kalita, J.C.; Dalal, D.C.; Dass, A.K. A class of higher order compact scheme for the unsteady two-dimensional convection-diffusion equation with variable convection coefficients. *Int. J. Numer. Methods Fluids* **2002**, *38*, 1111–1131. [CrossRef]
32. Karaa, S.; Zhang, J. High order ADI method for solving unsteady convection diffusion problems. *J. Comput. Phys.* **2004**, *198*, 1–9. [CrossRef]
33. Tian, Z.F.; Ge, Y. A fourth order compact ADI method for solving two dimensional unsteady convection diffusion problems. *J. Comput. Appl. Math.* **2007**, *198*, 268–286. [CrossRef]
34. Tian, Z.F. A rational high-order compact ADI method for unsteady convection diffusion equations. *Comput. Phys. Commun.* **2011**, *182*, 649–662. [CrossRef]
35. Sun, H.W.; Li, L. A CCD-ADI method for unsteady convection-diffusion equations. *Comput. Phys. Commun.* **2014**, *185*, 790–797. [CrossRef]
36. Karaa, S. A high-order compact ADI method for solving three-dimensional unsteady convection-diffusion problems. *Numer. Methods Partial Differ. Equ.* **2006**, *22*, 983–993. [CrossRef]
37. Cao, F.; Ge, Y. A high-order compact ADI scheme for the 3D unsteady convection diffusion equation. In Proceedings of the 2011 International Conference on Computational and Information Sciences, Chengdu, China, 21–23 October 2011; pp. 1087–1090.
38. Ge, Y.; Tian, Z.F.; Zhang, J. An exponential high order compact ADI method for 3D unsteady convection-diffusion problems. *Numer. Methods Partial Differ. Equ.* **2013**, *29*, 186–205. [CrossRef]
39. Ge, Y.; Zhao, F.; Wei, J. A high order compact ADI method for solving the 3D unsteady convection diffusion problems. *Appl. Comput. Math.* **2018**, *7*, 1–10. [CrossRef]
40. Lele, S.K. Compact finite difference schemes with spectral-like resolution. *J. Comput. Phys.* **1992**, *103*, 16–42. [CrossRef]
41. Wang, T.; Liu, T. A consistent fourth-order compact finite difference scheme for solving vorticity-stream function form of incompressible Navier-Stokes equations. *Numer. Math. Theory Methods Appl.* **2019**, *12*, 312–330.
42. Yang, X.; Ge, Y.; Zhang, L. A class of high-order compact difference schemes for solving the Burgers' equations. *Appl. Math. Comput.* **2019**, *358*, 394–417. [CrossRef]
43. Yang, X.; Ge, Y.; Lan, B. A class of compact finite difference schemes for solving the 2D and 3D Burgers' equations. *Math. Comput. Simul.* **2021**, *185*, 510–534. [CrossRef]
44. Zhanlav, T.; Chuluunbaatar, O.; Ulziibayar, V. Higher-order accurate numerical solution of unsteady Burgers' equation. *Appl. Math. Comput.* **2015**, *250*, 701–707. [CrossRef]
45. Hammad, D.A.; El-Azab, M.S. 2N order compact finite difference scheme with collocation method for solving the generalized Burger's-Huxley and Burger's-Fisher equations. *Appl. Math. Comput.* **2015**, *258*, 296–311. [CrossRef]
46. Chertock, A.; Epshteyn, Y.; Hu, H.; Kurganov, A. High-order positivity-preserving hybrid finite-volume-finite-difference methods for chemotaxis systems. *Adv. Comput. Math.* **2018**, *44*, 327–350. [CrossRef]
47. Chertock, A.; Kurganov, A.; Ricchiuto, M.; Wu, T. Adaptive moving mesh upwind scheme for the two-species chemotaxis model. *Comput. Math. Appl. Math.* **2019**, *77*, 3172–3185. [CrossRef]